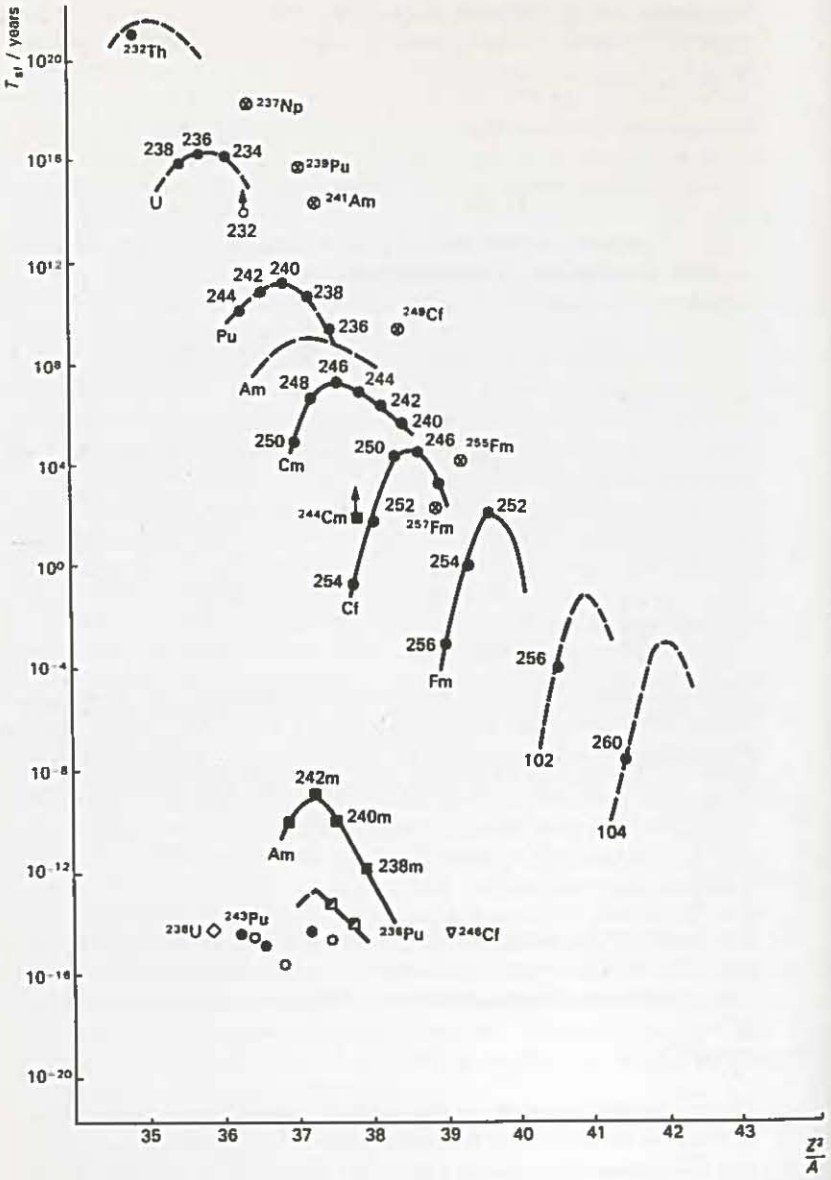

Figure 86 Plot of half-life for spontaneous fission against Z^2/A for heavy nuclides. Some shape isomers (see section 11.8) are included

11.5 Nuclear stability: large deformations

We now consider a nucleus whose fissionability parameter x is less than unity and which therefore has metastability against spontaneous fission. We wish to consider circumstances in which it suffers a deformation large enough for the long-range Coulomb forces to dominate the short-range nuclear forces which give rise to the surface energy. The nucleus will then proceed to undergo fission. The classical treatment of large deformations of a charged liquid drop is not in principle difficult but the mathematical complexities are very formidable. We can follow the procedure outlined in section 9.5.1 in connection with nuclear vibrations and express the deformed surface as a combination of spherical harmonics. The radius vector R will then be given by

$$R(\theta, \phi) = R\left[1 + \sum_{\lambda=1}^{\infty} \sum_{\mu=-\lambda}^{+\lambda} \alpha_{\lambda\mu} Y_{\lambda\mu}(\theta, \phi)\right].$$

In the face of the complications involved for completely general deformations, we limit consideration to the particular deformations in which $\mu = 0$ (which makes the radius vector independent of ϕ, and hence the surface is always that of a solid of revolution) and we take $\lambda = 2$ and $\lambda = 4$ as the only harmonics. These values of λ, as do all even values, lead to a shape which is symmetrical with respect to the xOy plane. This can be seen from Figure 87, in which are illustrated the cases $\lambda = 2, 3, 4$. We thus have for our deformed shape

$$R(\theta) = R[1 + \alpha_2 P_2(\cos\theta) + \alpha_4 P_4(\cos\theta)],$$

where $P_2(\cos\phi)$ and $P_4(\cos\phi)$ are as quoted in section 6.4. The next step is then to calculate the potential energy corresponding to different values of the two parameters α_2 and α_4 which are now being used to define the deformed shape. When this has been carried through, the result can be presented three-dimensionally, the energy plotted vertically against α_2 and α_4 plotted in the horizontal plane. To convey the situation two-dimensionally, we can plot contours as on a geographical map. The general form of the result can be seen in Figure 88. The spherical nucleus sits, as it were, in a bowl on an elevated plateau ringed around by mountains. There is a pass or saddle through these mountains to a lower plain lying beyond. This saddle represents the easiest (in the sense that least deformation energy is required) route from the original metastability of the nucleus to fission. The highest point in the pass is called the *saddle point*. It is found that at the saddle point the nucleus has not yet reached the point of separation into two parts although a waist has developed. The later stage when the separation is reached, is termed *scission point*.

More elaborate calculations introducing values of λ as large as $\lambda = 18$ have been carried through and the potential mapped out with higher accuracy. The form of the results remains the same. We therefore now have the picture of the

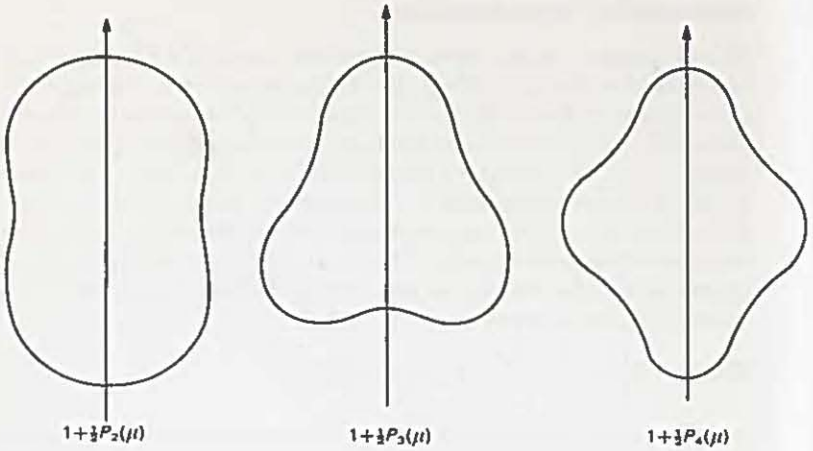

(a)

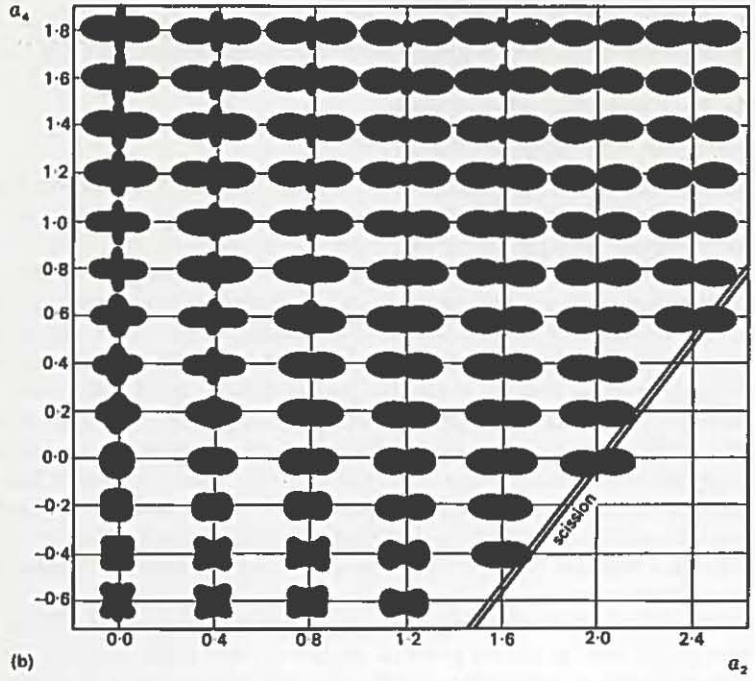

(b)

Figure 87 (a) Deformed spherical shapes comprising $\lambda = 2$, $\lambda = 3$ and $\lambda = 4$ deformations. Bodies are solids of revolution about the axes indicated. (b) Shapes of nuclear surfaces comprised of $\lambda = 2$ and $\lambda = 4$ deformations only. The figures possess rotational symmetry about the horizontal axis. The scission line is given by $\alpha_4 = -2{\cdot}5 + 1{\cdot}25\alpha_2$

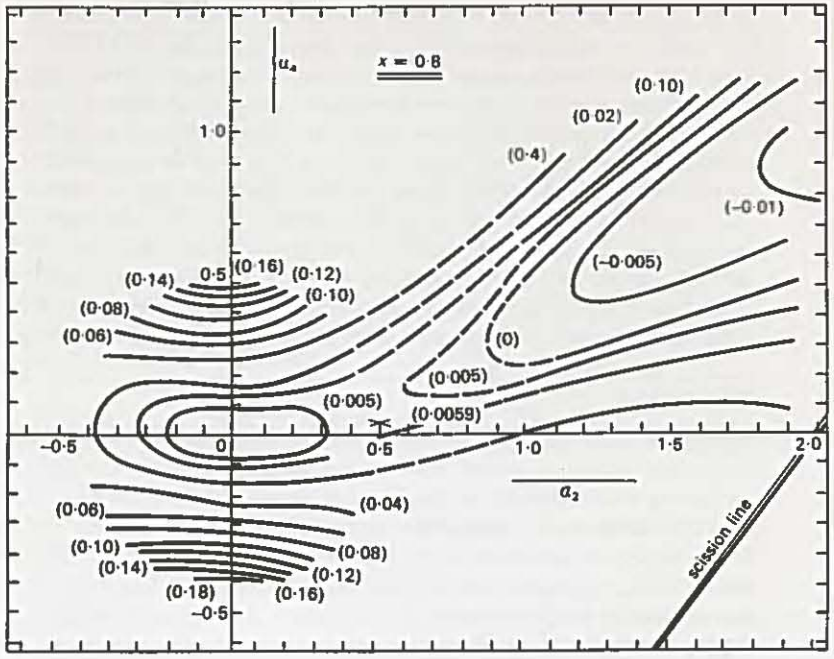

Figure 88 Contour map of potential energy of surface as a function of α_2 and α_4, all other αs being zero. Deformation energy is measured relative to spherical shape

nucleus being raised to an excited level by, let us say, neutron capture. This level will be in a region of high level density about 8 MeV above the ground state. The internal energy then has to be reorganized to deformation energy so that the nucleus takes up the shape appropriate to the saddle point. Thereafter it can pass back towards its original state or carry over towards scission.

11.6 Transition states

A. Bohr (1955) developed the idea that, the internal energy of the nucleus having been largely converted to energy of deformation and assuming that fission is taking place not too far above threshold, the nucleus will be 'cooled' at the saddle point. As a consequence its level structure will resemble that close to the ground state of a normal nucleus. Since it is highly deformed it should be expected to show collective rotational levels. In proceeding from the ground state to the scission point, the nucleus will have to go through the 'ground state' or one of the comparatively small number of collective levels at the saddle-point, levels which

are said to be associated with *transition states*. The number of available transition states will control the rate at which fission proceeds and the spins associated with these states will impose angular-momentum conditions on the system. The concept of transition states has proved very fertile and there is good evidence for their existence. For example, the fission cross-section as a function of excitation energy of the fissile nucleus shows a series of plateaux which can be interpreted as corresponding to a succession of new transition states entering the process. Further, a value of K, the spin about the symmetry axis of the deformed nucleus (see section 9.4), can be investigated by studying the angular distribution of the fission fragments (which will be emitted along the symmetry axis) when the spin of the system is aligned in a nuclear alignment experiment or can be determined from the kinematics in the case of fission induced by a beam of energetic particles.

11.7 Scission point

No convincing theoretical description is yet available of the scission process, i.e. the final tearing of nuclear matter as the fragments separate. The details of the tearing will decide whether the fission is binary, ternary or involves more than three products. A considerable amount of experimental evidence for ternary fission has now accumulated. If we take the extreme (but not customary) view of regarding the neutron as a fission fragment, then two fission fragments plus a neutron strictly would constitute 'ternary fission'. A study of the angular distribution of prompt neutrons with respect to the direction of the main fission fragments reveals that a proportion of the neutrons are emitted isotropically. These are the ternary neutrons. The non-isotropic neutrons will be those emitted, following scission, from the recoiling fragments. Light charged fragments have also been observed to be emitted at scission. We noted in section 11.2 that of a thousand fission events about two or three involved the emission of an α-particle in addition to the main fragments. In Table 8 the relative frequency of occurrence of fission accompanied by the emission of other charged fragments is shown. The figures relate to long-range particles emitted by ^{252}Cf decaying by spontaneous fission.

Evidence for 'true' ternary fission involving the emission of three equal fragments has been sought by looking for coincidences in counters set to detect three coplanar fragments emitted in directions 120° apart. The results of this difficult experiment are claimed to establish that the rate of 'true' ternary fission to binary fission is about 10^{-6} in ^{240}Pu* and ^{242}Pu*. This experiment also indicated that the fission fragment masses lay in the ranges 30-40 a.m.u. and 50-60 a.m.u. However, careful radiochemical examination has not confirmed the presence of the predicted amounts of material with these mass values in the fission fragments. The occurrence of 'true' ternary fission, which is a matter of great importance for fission theory, is therefore in our present state of knowledge an open question.

Finally, we note that there is no satisfactory theoretical explanation available of the asymmetric distribution of mass between the fission fragments. If the deformation could be treated in full generality and not subject to the restrictions

Table 8 Long-Range Particles Emitted in Spontaneous Fission of ^{252}Cf

Particle	*Measured relative intensity*	*Most probable energy*/MeV	*High-energy cut-off*/MeV
Proton	$1{\cdot}10 \pm 0{\cdot}15$	$7{\cdot}8 \pm 0{\cdot}8$	18·8
Deuteron	$0{\cdot}63 \pm 0{\cdot}03$	$8{\cdot}0 \pm 0{\cdot}5$	22·4
Triton	$6{\cdot}42 \pm 0{\cdot}20$	$8{\cdot}0 \pm 0{\cdot}3$	24·5
^{3}He	$< 7{\cdot}5 \times 10^{-2}$		
^{4}He	100	$16{\cdot}0 \pm 0{\cdot}2$	37·9
^{6}He	$1{\cdot}95 \pm 0{\cdot}15$	$12{\cdot}0 \pm 0{\cdot}5$	32·6
^{8}He	$(6{\cdot}2 \pm 0{\cdot}8) \times 10^{-2}$	$10{\cdot}2 \pm 1{\cdot}0$	28·7
Li ions	$0{\cdot}126 \pm 0{\cdot}015$	$20{\cdot}0 \pm 1{\cdot}0$	38·0
Be ions	$0{\cdot}156 \pm 0{\cdot}016$	$\sim 26{\cdot}0$	45·0

introduced above, and if the transition states were fully understood, then an explanation might be forthcoming within the framework of the theory sketched above.

11.8 Shape isomerism

The adequacy of the above theory was put in doubt by the discovery in 1962 of an isomeric state in ^{242}Am which decayed by spontaneous fission with a half-life of 14 ms. The ground state of ^{242}Am is believed to have a spontaneous-fission of half-life of the order of 10^{10} years. No satisfactory explanation could be given in terms of the theory of the speed at which spontaneous fission proceeded from the isomeric state and why it was so much more favoured than α-decay. Strutinsky (1969) (for further information see L. Wilets, *Theories of Nuclear Fission*, Clarendon Press, 1964) has proposed an elaboration of fission theory which provides an explanation of the behaviour of this isomeric state and of many others which have been subsequently found. It also opens up other theoretical and experimental possibilities.

We recall that the liquid-drop model predicted a smooth variation of nuclear binding energy with A-value, which was in broad agreement with the measured binding energies. This smooth curve was found however to be 'modulated' by effects of shell corrections. In particular, at Z- and N-values corresponding to closed shells we saw that there was a marked increase in binding energies. The shell correction is related to the single-particle level density in the neighbourhood of the highest occupied levels in the single-particle level scheme. The correction is greatest when the level density is low. Thus, for spherical nuclei with closed shells and degenerate levels, the effect is most marked.

It will be appreciated from Figure 61 (p. 170) that the level density determining the shell correction will not only differ from one nucleus to another but will, in the case of a particular nucleus, change with the nuclear deformation. From the Nilsson diagram of Figure 61 it can be seen that the level density can go through a minimum for a deformation greater than the ground-state deformation. Thus the

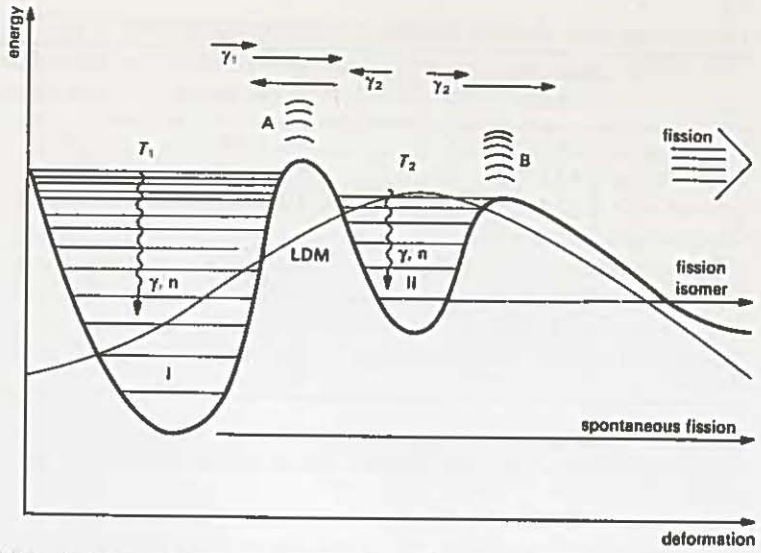

Figure 89 Potential energy against deformation showing second minimum. As well as excited states within the first well (I), note the transition states at A and B and the intermediate states in the second well (II). The liquid-drop model prediction is also shown

shell correction, according to Strutinsky's calculations, can be positive or negative for the same nucleus depending on the deformation. This has the effect of modifying the curve of Figure 85 (p. 223) so that it has, as shown in Figure 89, a second minimum. If this shape has validity then we can associate the isomeric spontaneous fissioning state with a nucleus deformed beyond the first saddle point and situated in the second potential minimum. On this view, the phenomenon has been termed *shape isomerism*. From this isomeric state the nucleus may return to the first minimum or it may proceed to the scission point, barrier penetration being involved in both eventualities. If the second well is deep enough there will then be the possibility of a system of excited states based on this deformed nucleus. These states are referred to as *intermediate states*.

Many cases of shape isomerism have now been found. In the nucleus ^{240}Pu there appear to be two such isomeric states, one with a half-life of 30 ns and the other with a half-life of 5 ns. The existence of the second potential minimum is thus thought to be a general characteristic of the fissile nuclei.

There is interesting evidence for the existence of intermediate states in the behaviour of the neutron-capture cross-section in ^{239}Pu at low neutron energies. Very many resonances are found in neutron capture, only a few of which give rise to fission. These resonances, shown in Figure 90, which lie below the so-called 'threshold' for fission, are now interpreted as arising when the position of

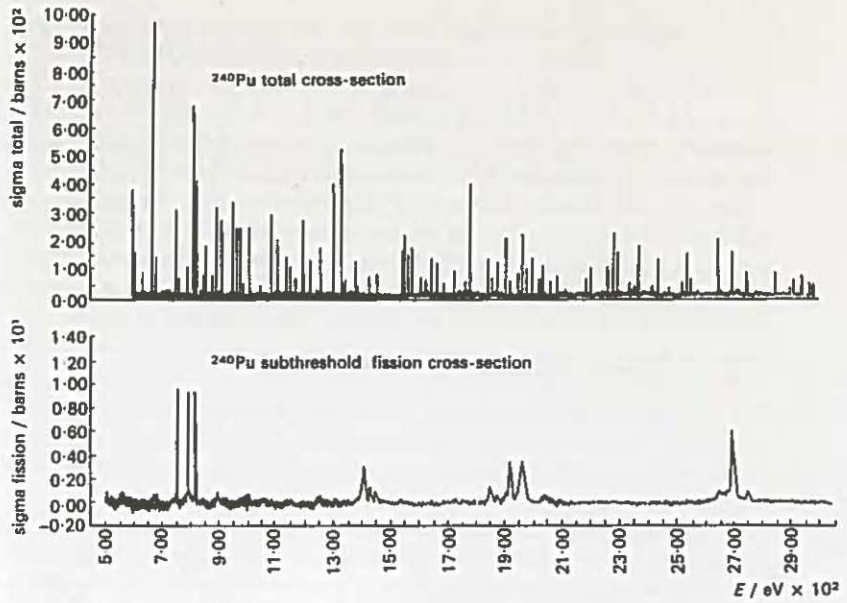

Figure 90 The cross-section for capture of neutrons in ^{240}Pu for all the processes which can occur and the cross-section for capture leading to fission. The grouping of the fission resonances is associated with the intermediate states at the second minimum

the compound nuclear level in the first well lies at the same height as an intermediate level in the second well.

11.9 Superheavy nuclei

These recent theoretical developments have not only provided explanations of previously puzzling aspects of the fission process in the region $Z \simeq 90, A \simeq 240$ but have encouraged speculation about the possible existence of *superheavy nuclei*. As we saw in section 11.4, the liquid-drop model predicts that for nuclei with $Z^2/A > 44$ fission instability should set in. However, shell corrections in uranium and plutonium, neither of which is a magic nucleus, confer greater stability than would have been anticipated. It has therefore been suggested that perhaps in heavier nuclei which are magic or near magic in both proton and neutron numbers, the shell correction can be large enough to restore some measure of stability against spontaneous fission. Following this suggestion we note that the next magic number for protons on the single-particle model would be 126. However, theoretical considerations suggest that there may be large shell corrections in a somewhat lower range of Z-values namely 114 to 120. Above 126 the next single-particle magic number is 184. Values of Z around 114 and N around 184 have then been considered as defining an island on the nuclear chart in which nuclei of short but measurable (or perhaps even quite long) half-life, the

so called *superheavy nuclei* might exist. They are expected theoretically to be relatively stable against β-decay. Calculations have been performed in an attempt to arrive at estimates of half-lives against α-decay and spontaneous fission. The fierce dependence of half-life on potential barrier, and the large extrapolation involved in calculating the shell correction, would unfortunately permit any half-life ranging from nanoseconds to millions of years to be accommodated.

The prospect, however nebulous, of extending the region of stability or quasi-stability on the nuclear chart has aroused considerable interest. A method for producing superheavy nuclei in the laboratory that has been proposed is the bombardment of a uranium target by uranium ions accelerated to an energy of about eight million electronvolts per nucleon. This might lead to the reaction

$$^{238}_{92}\mathrm{U} + {}^{238}_{92}\mathrm{U} \rightarrow {}^{298}_{114}\mathrm{SH} + {}^{174}_{70}\mathrm{Yb} + 4\mathrm{n}.$$

The accelerators necessary for such experiments do not at present exist. The prospect of the production of superheavy nuclei is one of the main arguments put forward to justify the development of larger and more sophisticated heavy-ion accelerators.

Should superheavy nuclei be found with lifetimes long enough to permit the measurement of their properties, it is interesting to note that not only would they be of outstanding interest as new forms of nuclear matter but they would open up new fields of atomic physics. The binding energy of the K-electron in uranium, about 114 keV, is still quite small compared to the 1 MeV gap between the positive and negative energy states of the electron. For the superheavy nuclei the K-electrons would lie much deeper, $Z/137$ would be appreciably closer to unity and certain approximations quite satisfactory for known nuclei would have to be reconsidered. If it ever became possible to produce and study nuclei with $Z > 137$ then the electrodynamics of the K-shell would be expected to be very different from that of the nuclei at present known.

11.10 Summary

The challenge of the experimental facts of spontaneous and induced fission has led to a theory for the behaviour of a grossly deformed nucleus. Basically liquid drop in structure, it has had collective states and shell corrections now built into it. A second minimum occurs in the potential energy against deformation curve and indicates how important the shell corrections can be. It has been conjectured that these corrections may be large enough in the neighbourhood of higher magic neutron and proton numbers to lead to superheavy nuclei long enough lived to be identified. Experimental exploration of these suggested 'islands of stability' lying off the known 'peninsula' of stable nuclides awaits the development of accelerators capable of accelerating ions much heavier than those that can be accelerated in presently existing machines.

Appendix A
Ground State Properties of Stable Nuclei

	A	*Z*	*N*	*I*	π	*SM***	μ‡	*Q*§	*M* − *A*¶	*Percentage abundance*
n	1	0	1	$\frac{1}{2}$	+		−1·9131		+8·071 44	
H	1	1	0	$\frac{1}{2}$	+	$s_{\frac{1}{2}}$	+2·792 78		+7·288 99	99·985
	2	1	1	1	+	$(\frac{1}{2},\frac{1}{2})$	+0·857 42	+0·0028	+13·136	0·015
He	3	2	1	$\frac{1}{2}$	+	$s_{\frac{1}{2}}$	−2·1276		+14·931	0·00013
	4	2	2	0	+				+2·425	100
Li	6	3	3	1	+	$(\frac{3}{2},\frac{3}{2})$	+0·822 02	−0·0008	+14·088	7·4
	7	3	4	$\frac{3}{2}$	−	$p_{\frac{3}{2}}$	+3·2564	−0·04	+14·907	92·6
Be	9	4	5	$\frac{3}{2}$	−	$p_{\frac{3}{2}}$	−1·1776	+0·05	+11·350	100
B	10	5	5	3	+	$(\frac{3}{2},\frac{3}{2})$	+1·8007	+0·08	+12·052	18·8
	11	5	6	$\frac{3}{2}$	−	$p_{\frac{3}{2}}$	+2·6885	+0·04	+8·668	81·2
C	12	6	6	0	+				0 (standard)	98·89
	13	6	7	$\frac{1}{2}$	−	$p_{\frac{1}{2}}$	+0·7024		+3·125	1·11
N	14	7	7	1	+	$(\frac{1}{2},\frac{1}{2})$	+0·4036	+0·01	+2·864	99·63
	15	7	8	$\frac{1}{2}$	−	$p_{\frac{1}{2}}$	−0·2831		+0·100	0·37
O	16	8	8	0	+				−4·737	99·759
	17	8	9	$\frac{5}{2}$	+	$d_{\frac{5}{2}}$	−1·8937	−0·026	−0·808	0·037
	18	8	10	0	+				−0·782	0·204
F	19	9	10	$\frac{1}{2}$	+		+2·6288		−1·486	100
Ne	20	10	10	0	+				−7·041	90·8
	†21	10	11	$\frac{3}{2}$	+	$(d_{\frac{5}{2}})^3$	−0·6618	+0·09	−5·730	0·26
	22	10	12	0	+				−8·025	8·9
Na	†23	11	12	$\frac{3}{2}$	+	$(d_{\frac{5}{2}})^3$	+2·2175	+0·14	−9·528	100
Mg	24	12	12	0	+				−13·933	78·8
	25	12	13	$\frac{5}{2}$	+	$d_{\frac{5}{2}}$	−0·8551	+0·22	−13·191	10·1
	26	12	14	0	+				−16·214	11·1

** Shell-model configurations.
‡ Nuclear magnetic dipole moment in nuclear magnetons.
§ Nuclear electric quadrupole moment in barns.
¶ Mass excess (see section 5.8) in MeV.